

Earth's Future

RESEARCH ARTICLE

10.1029/2020EF001671

Special Section:

Fire in the Earth System

Key Points:

- Empirical evidence-based statistical approach is employed to assess the causes of the 2019–2020 bushfire in the NSW state of Australia
- Drought, soil moisture, wind speed, relative humidity, heat waves, fuel moisture, and certain land cover types drive bushfires
- Slope did not contribute in bushfire occurrence and propagation

Correspondence to:

H. Moradkhani,
hmoradkhani@ua.edu

Citation:

Deb, P., Moradkhani, H., Abbaszadeh, P., Kiem, A. S., Engström, J., Keellings, D., & Sharma, A. (2020). Causes of the widespread 2019–2020 Australian bushfire season. *Earth's Future*, 8, e2020EF001671. <https://doi.org/10.1029/2020EF001671>

Received 16 JUN 2020

Accepted 24 OCT 2020

Accepted article online 3 NOV 2020

Author Contributions:

Conceptualization: Proloy Deb

Data curation: Hamid Moradkhani

Formal analysis: Proloy Deb, Johanna Engström

Methodology: Proloy Deb, Hamid Moradkhani, Peyman Abbaszadeh

Supervision: Hamid Moradkhani,

Anthony S. Kiem, Ashish Sharma



Visualization: Peyman Abbaszadeh, David Keellings

Writing - original draft: Proloy Deb, David Keellings, Ashish Sharma
(continued)

©2020. The Authors.

This is an open access article under the terms of the Creative Commons Attribution-NonCommercial-NoDerivs License, which permits use and distribution in any medium, provided the original work is properly cited, the use is non-commercial and no modifications or adaptations are made.

Causes of the Widespread 2019–2020 Australian Bushfire Season

Proloy Deb^{1,2} , Hamid Moradkhani^{1,2} , Peyman Abbaszadeh^{1,2} , Anthony S. Kiem³ , Johanna Engström¹ , David Keellings^{1,4} , and Ashish Sharma⁵ 

¹Center for Complex Hydrosystems Research (CCHR), University of Alabama, Tuscaloosa, AL, USA, ²Department of Civil, Construction and Environmental Engineering, University of Alabama, Tuscaloosa, AL, USA, ³Centre for Water, Climate and Land (CWCL), School of Environmental and Life Sciences (Earth Sciences), University of Newcastle, Callaghan, NSW, Australia, ⁴Department of Geography, University of Alabama, Tuscaloosa, AL, USA, ⁵School of Civil and Environmental Engineering, University of New South Wales, Sydney, NSW, Australia

Abstract The recent bushfires (2019–2020) in New South Wales (NSW) Australia were catastrophic by claiming human and animal lives, affecting ecosystems, destroying infrastructure, and more. Recent studies have investigated relationships between hydroclimatic signals and past bushfires, and very recently, a few commentary papers claimed drought and fuel moisture content as the probable causes for the widespread 2019–2020 bushfires. Therefore, in this study, a novel work of encompassing a wide range of factors attributing to the recent bushfires is presented. Empirical evidence-based statistical methods are used to identify the hydroclimatic variables and geomorphic characteristics contributing to the 2019–2020 bushfires. The results highlight that ongoing drought, surface soil moisture (SSM), wind speed (WS10), relative humidity (RH), heat waves (HW), dead and live fuel moisture, and certain land cover types create favorable conditions for fire ignition and aid in fire propagation in different regions of the NSW state. The findings suggest that accounting for the above-identified variables in bushfire prediction and monitoring system are crucial in avoiding such catastrophes in the future. The overarching application of this study is developing robust and more versatile fire protection planning and management.

Plain Language Summary Since the 2019–2020 Australian bushfires were catastrophic in terms of burnt area and severity, a detailed analysis of the primary causes is crucial. In this paper, several probable causes are tested statistically to establish their relationship with the burnt area. The results indicate that the ongoing drought, surface soil moisture, wind speed, relative humidity, heat waves, dead and live fuel moisture, and land cover with certain vegetation (particularly native eucalyptus and grazing land) are the primary causes of the widespread bushfire. These results are extremely critical in updating the current bushfire planning and management.

1. Introduction

Bushfires (also known as wildfires) are a common and natural phenomenon which play a vital role in the atmospheric and terrestrial system (Bowman et al., 2009). Globally on average, an approximate area of 350 Mha is burnt annually (Giglio et al., 2013). This phenomenon is of no exception for the driest continent in the world that is Australia, where it occurs regularly, and has contributed to the evolution of the continent over millions of years. Several mega bushfire events in Australia have been documented such as Gippsland fires and Black Sunday (1926), Black Friday (1939), Australian Bushfire Season (1974–1975), Waterfall bushfire (1980), Canberra bushfires (2003), and Black Saturday (2009) (Weber et al., 2019). However, the recent bushfire season (2019–2020) in Australia, centered in the southeastern part of the country (New South Wales, NSW), has turned out to be the most catastrophic (in terms of burnt area and severity) in the continent's history since the European settlement and colloquially also known as the Black Summer. It has claimed 28 human lives (Roach, 2020), over 1.25 billion animal lives (TV10, 2020), damaged over 3,000 homes (Yeung, 2020) and caused an economic loss of over \$110 billion (until January 2020) (Roach, 2020).

Existing studies have indicated that the primary cause of flame occurrence is the combination of three main components: hot weather, fuel availability, and an ignition source (Moritz et al., 2005). Additionally, with

Writing – review & editing: Hamid Moradkhani, Anthony S. Kiem, Johanna Engström

progressive availability of vegetation (fuel) in the path of fire accompanied by high temperature and wind speed and low precipitation, the fire accelerates and has consequently led to major bushfire incidents in the past (Bessie & Johnson, 1995; Littell et al., 2009; Nolan et al., 2016b). Climate change has already induced an increase in temperature of approximately 0.5°C per decade since 1980s in NSW State of Australia (Heritage, 2014). This increase in temperature has already influenced the water cycle by intensifying the localized precipitation at some regions (Marvel & Bonfils, 2013) and simultaneously aggravating the drought intensity and frequency at other locations (Dai, 2013; Deb et al., 2019). Intense precipitation events have the ability to transform barren lands into widespread herbaceous plants and thus increasing fuel availability (O'Donnell et al., 2011). Similarly, major droughts create favorable conditions for bushfires in forested ecosystems (Bradstock et al., 2014). In addition, natural climatic variability has been linked to seasonal-decadal long droughts in various regions (Forootan et al., 2019; Kiem & Franks, 2004). Furthermore, sea surface temperature alterations are also claimed to have strong associations with regional droughts (Harrison et al., 2019; Wu & Kinter, 2009) which further governs the spread of bushfires (Russo et al., 2017).

A plethora of studies have investigated the underlying causes of widespread bushfires covering different climatic regions of the world. The majority of these studies have only considered local climatic factors, particularly, temperature, wind speed, relative humidity, and meteorological droughts which control the ignitability and spread of fire (Clarke et al., 2013; Flannigan et al., 2009, 2013; Russo et al., 2017). A handful of studies have focused on the effect of slope on fire propagation (Butler et al., 2007; Estes et al., 2017; Liu et al., 2014) and fuel moisture content (Burton et al., 2019). Only a few of these variables (particularly, temperature, relative humidity, wind speed, and meteorological drought) are accounted for in the McArthur Forest Fire Danger Index (FFDI) (Noble et al., 1980), which is widely used to assess the probability of bushfire occurrence in Australian landscapes (Verdon et al., 2004). Apart from these factors, some studies have also found antecedent soil moisture content to be a critical factor governing the bushfire propagation; however, these studies are only conducted in the United States of America (Krueger et al., 2015; Schulte et al., 2019). Also, past research studies have illustrated that some of the major historical bushfire events in the Southeast Australian region have proliferated due to extreme heat waves (Alexander & Arblaster, 2009; Karoly, 2009).

Given that the fire swept unusual and record breaking areal extent, it gained extreme interest of the bushfire research community. One of the correspondence papers by Boer et al. (2020) investigated satellite images of the recent bushfire and concluded “temperate broadleaf and mixed” forest biome was more susceptible to the 2019–2020 bushfires. Similarly, in a commentary by King et al. (2020), the wide extent of the bushfires is claimed due to extremely dry conditions that persisted over the past 2 years. These dry conditions were further linked to negative Indian Ocean Dipole (IOD) and absence of La Niña. Sanderson and Fisher (2020) commented that the 2019–2020 Australian bushfire is an indication of the future that is quickly becoming present and this is solely due to climate change. Furthermore, Nolan et al. (2020) explained in a Letter that dry fuel moisture and the ongoing droughts are the only causes of the 2019–2020 Australian bushfires. A comment on this Letter by Ambadan et al. (2020) discussed that precipitation deficit is the primary cause of the bushfire. Additionally, they also claimed fuel loads were casual, given that the fuel availability among unburnt and burnt areas/forests were the same. This comment was further counter argued by Bradstock et al. (2020) as speculative and not supported by any scientific evidence or data analysis.

Evidently, recent studies have explored only a few of the most probable causes of the bushfires. Also, the abovementioned studies have explored the implication of each variable on bushfire independently. To the best of our knowledge, there is no comprehensive study in the existing literature yet, which has considered most, if not all possible variables either individually or in combination governing the widespread bushfires, which is also the novelty of this study. The overarching aim is to investigate all possible variables that contributed to the extensive bushfires in NSW State of Australia. In this paper, an empirical analysis is conducted while accounting for all potential causes, which may have triggered the bushfires. Here the analysis focusses on the period of September to December 2019, given the extensive area burnt during these months instead of October–February months, when usually the bushfire severity (both intensity and burnt area) is at its peak. The approach employed in this study is to explore whether the bushfire-affected areas (called bushfire units or BFU, used hereafter) are associated with any particular hydroclimatic or geomorphic variable (i.e., are the BFUs more likely to inherit/experience certain fire-causing factors). The findings of this study are useful in developing better bushfire prediction tools and management plans.

Table 1
Data Source, Format, Temporal, and Spatial Resolution Used in This Study

Data	Source	Format	Temporal resolution	Spatial resolution
BFU	NSW Rural Fire Service	Shapefile	-	-
SSM	Australian Water Resource Assessment Landscape (AWRA-L), CSIRO, and BoM (http://www.bom.gov.au/water/landscape/#/sm/Actual/day/-28.4/130.4/3/Point///2020/6/3/)	NetCDF	Daily	0.05°
WS10	NCEP/NCAR Reanalysis data (https://www.esrl.noaa.gov/psd/data/gridded/data.ncep.reanalysis.pressure.html)	NetCDF	Daily	0.05°
RH	SILO Data Drill (https://www.longpaddock.qld.gov.au/silo/) (Jeffrey et al., 2001)	NetCDF	Daily	0.05°
6-Month SPEI	Global SPEI database (https://spei.csic.es/database.html)	NetCDF	Monthly	0.5° (regridged to 0.05°)
Vapor Pressure Deficit	SILO Data Drill (https://www.longpaddock.qld.gov.au/silo/)	NetCDF	Daily	0.05°
VARI	MOD09A1v006 (https://lpdaac.usgs.gov/products/mod09a1v006/)	NetCDF	8-day	0.005°
Maximum Temperature (to Calculate HW)	SILO Data Drill (https://www.longpaddock.qld.gov.au/silo/)	Raster	Daily	0.05°
LULC	NSW Department of Planning, Industry, and Environment	Raster	-	0.01°
DEM (for Slope Calculation)	Geoscience Australia	Raster	-	30 m

2. Data Sets and Preprocessing

In this analysis, nine different variables are considered to identify their influence on the bushfires. These variables are 5-day lag surface soil moisture (SSM) (10 cm), average daily wind speed at 10 m height (WS10) (calculation in section 2.1), average daily relative humidity (RH) (%), 6-month Standardized Precipitation Evapotranspiration Index (SPEI), heatwave (HW) (derived from daily maximum temperature; section 2.2), daily dead fuel moisture (%) (derived from vapor pressure deficit; section 2.3 for details), live fuel moisture (%) (calculated from Moderate Resolution Imaging Spectroradiometer (MODIS); details in section 2.4), average BFU slope (derived from 30 m digital elevation model), and land use land cover (LULC). Gridded information (at different spatial scales, ranging from ~0.005° to 0.5°) is available for all the variables and their details are provided in Table 1. Additionally, BFU characteristics including date, number of days with active fire, and area burnt are obtained from NSW Rural Fire Service (NSW RFS) in the format of shapefile polygons, called BFUs here (Figure 1). The BFUs are grouped into five zones north (NO), northeast (NE), central (CE), southeast (SE), and southwest (SW) as shown in Figure 1, for the convenience of representing the results.

Since the bushfire incidents occurred on different dates at the BFUs, daily WS10, RH, and vapor pressure deficit (used to calculate dead fuel moisture) are retrieved only for the days of bushfire for each BFU. Also, following the suggestion of Ambadan et al. (2020), SSM data is collected for 5 days prior to bushfire incidents at each BFU. Live fuel moisture is calculated based on the available date of MODIS data set (MOD09A1) prior to the starting date of the bushfire at each BFU. For spatial consistency, these gridded data sets are first regrided to 0.05° using a bilinear approach, followed by spatially averaging at BFU scale to conduct further analysis. The time variant variables, that is, WS10, RH, and vapor pressure deficit are temporally averaged from daily to number of days with active bushfire at each BFU to represent the average values over the bushfire period. Similarly, SPEI is processed at seasonal scale where each pixel depicts seasonal average of 6-month SPEI value for the months of September to December. These values are ultimately spatially averaged at BFU scale. The 6-month SPEI is considered following the findings of Nolan et al. (2020), where long-term drought indices are emphasized for the Australian context due to its high prevalence.

2.1. Calculation of WS10

Since the wind speed information is available in its zonal and meridional components (U and V, respectively), the daily absolute wind speed value is calculated by using Equation 1.

$$WS10 = \sqrt{U^2 + V^2} \quad (1)$$

where WS10 is the absolute wind speed at 10 m height (ms^{-1}) and U and V are the zonal and meridional velocity of wind in ms^{-1} . The daily WS10 is calculated for each pixel and is spatially averaged for each

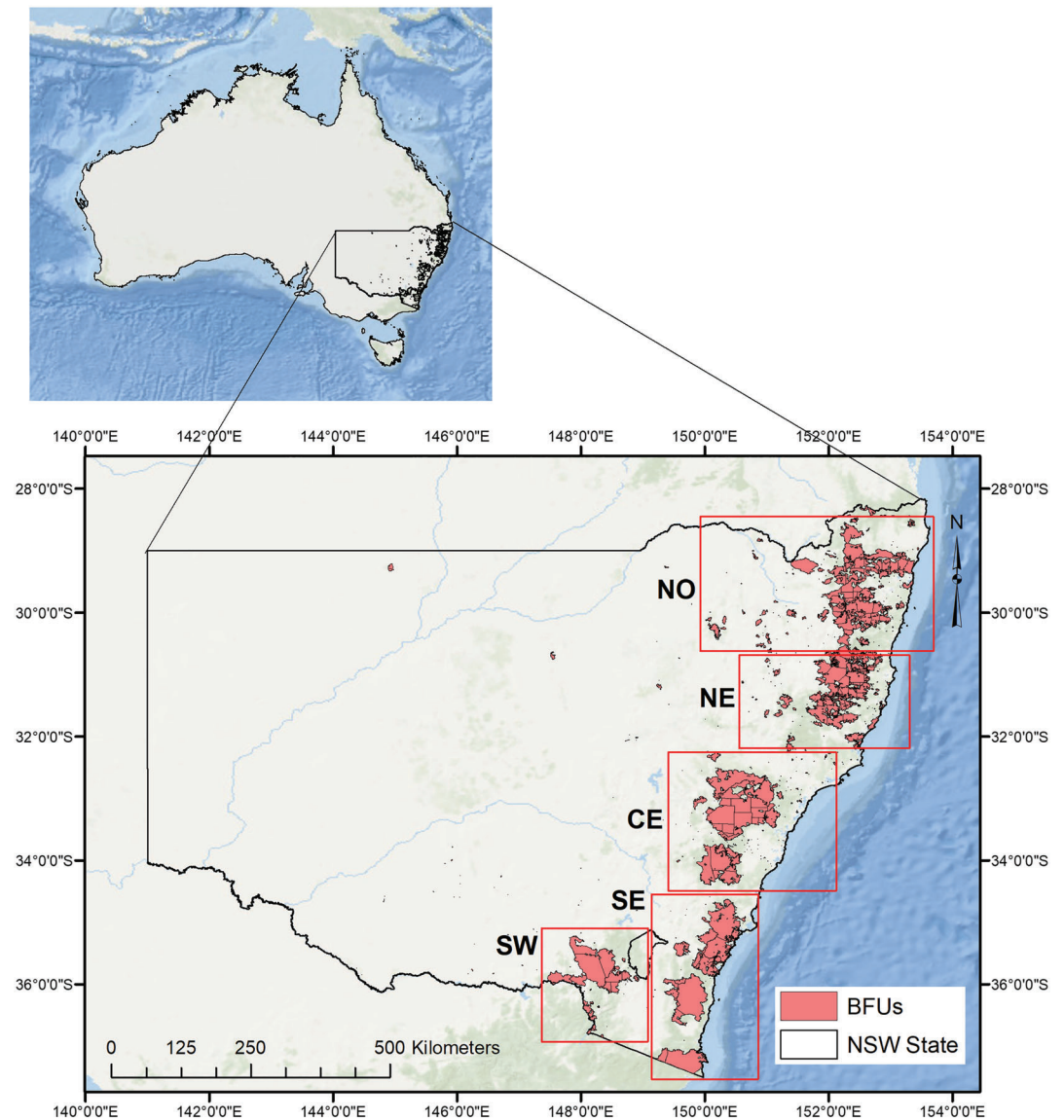


Figure 1. New South Wales state in Australia highlighting the Bush Fire Units (BFUs) used in this study. Note that the red rectangles represent the regions which are used in the study for the convenience of discussion of results; northern, northeastern, central, southeastern and southwestern BFUs are represented by NO, NE, CE, SE, and SW, respectively. Data source: NSW Rural Fire Service.

BFU for the days of bushfire incidents at each BFU. This means in the analysis, even for adjacent BFUs, they have different days of wind speed values only for the days when there is a bushfire incident. These wind speed values are temporally averaged for the duration of bushfires to represent the average wind speed for the bushfire period at each BFU.

2.2. Calculation of HW

In this study, a HW is defined as an event with a period of at least 3 consecutive days with maximum daily temperature exceeding the 95th percentile of the maximum temperature for the historical period (1951–2005). The HW is calculated at each pixel for the bushfire season (i.e., September to December 2019) and if HW events are identified (even if it is only one incidence), each pixel is assigned “1,” otherwise “0.” This approach is robust and is widely used at global scale studies for calculating heat waves (Dosio, 2017; Russo et al., 2014).

2.3. Calculation of Dead Fuel Moisture

In this study, dead fuel moisture is calculated considering the suspended fuel in the 10 h fuel class (6.35–25 mm diameter). The semimechanistic model developed for Australia by de Dios et al. (2015) is employed in this study. The dead fuel moisture model is based on an exponential relationship among the dead fuel moisture and vapor pressure deficit. The model is given in Equation 2.

$$\text{Dead FM (\%)} = 6.79 + 27.43e^{(-1.05D)} \quad (2)$$

where Dead FM is dead fuel moisture in percentage and D is vapor pressure deficit in kPa. Temporal and spatial averaging of dead fuel moisture for active bushfire days and at BFU scale respectively is done following the procedure of WS10 explained in section 2.1. This model was also employed in other studies in Australia continent such as Nolan et al. (2016a, 2016b).

2.4. Calculation of Live Fuel Moisture

The live fuel moisture is basically the ratio of mass of water within the fuel to oven-dry weight of fuel. It is calculated from the MODIS Terra satellite product MOD09A1, following the approach of Caccamo et al. (2012). In order to calculate the live fuel moisture, first the visible atmospherically resistant index (VARI) is calculated from the 8-day composite data set using the approach of Gitelson et al. (2002) and is given in Equation 3.

$$\text{VARI} = \frac{\text{band 4} - \text{band 1}}{\text{band 4} + \text{band 1} - \text{band 3}} \quad (3)$$

As mentioned earlier, only the day with available data prior to the bushfire incident at a BFU is considered in this analysis. Post calculation of VARI, live fuel moisture is calculated using the Equation 4.

$$\text{Live FM (\%)} = A \times e^{B \times \text{VARI}} \quad (4)$$

where Live FM is live fuel moisture in percentage and A and B are constants and the above equation needs to be calibrated. Nolan et al. (2016b) conducted an exclusive study over the southeastern Australia and calibrated A and B parameters as 52.51 and 1.36, respectively, which are adopted in this study. Live fuel moisture is calculated for each pixel of 500 m (~0.005°), then it is regridded to 0.05° and finally spatially averaged for each BFU.

3. Methods

As mentioned earlier, time variant variables, that is, WS10, RH, and dead fuel moisture are averaged both spatially at BFU scale and temporally for only the days of bushfire incidents at each BFU. This led to only one value of these variables at each BFU. Similarly, for the case of 6-month SPEI, SSM, live fuel moisture, and number of HW and slope have only one value for each BFU. Postcalculation of these variables, bushfire duration average values of WS10, RH, 6-month SPEI, and dead fuel moisture are compared against BFU “areas” (in ha) using the two-sample Kolmogorov-Smirnov (KS) test of cumulative distributions. In other words, for WS10, if $x_1, x_2, x_3, \dots, x_n$ represent spatial and bushfire duration average WS10 values (in ms^{-1}) for $\text{BFU}_1, \text{BFU}_2, \text{BFU}_3, \dots, \text{BFU}_n$, respectively, they are compared against $y_1, y_2, y_3, \dots, y_n$ representing BFU areas in ha. Similarly, SSM, live fuel moisture, slope, and number of HW events within each BFU are compared against BFU area using the two-sample KS test. In order to determine which particular land use type is more associated with bushfires, Kendall rank correlation coefficient (τ) is calculated for each land use class among the number of pixels within each BFU and the BFU area. The tests are done at a significance level of 0.05 with the null hypothesis in the KS test as: samples derived from the two data sets follow the same distribution. The BFUs with area smaller than the pixel size are ignored in the analysis. In this study, both the two-sample KS test and the Kendall rank correlation coefficient are used since they are nonparametric and are insensitive to nonnormal distributions.

Since spatial studies are susceptible to spatial correlation among variables, any statistical tests conducted (for example two-sample KS test here) on the variables may lead to erroneous outcomes. The conventional approach to avoid this is by conducting joint significance of multiple statistical tests (either “field” or

Table 2
Two-Sample KS Test Result for the Variables Compared Against BFUs
(Bold *p* Values Indicate Statistically Significant Values)

Variables	Two-sample KS test <i>p</i> value
SSM	0.068
WS10	0.125
RH	0.116
SPEI	0.068
HW	0.097
Dead Fuel Moisture	0.113
Live Fuel Moisture	0.072
Average BFU Slope	0.011

“global” significance tests). In this approach, the number of “local” tests resulting in the nominally significant results are counted, following which the judgment is done based on the context of the counts of the distributions if all the local null hypotheses are true. The major challenge with this approach is that the test results are sensitive to the nature of the test statistic. Also, this approach ignores the confidence level at which the locally significant test statistics reject the null hypothesis (Ivanov et al., 2018). To overcome this, “false discovery rate” (FDR) approach is more suitable where identification of locally significant tests is done by controlling FDR. Basically, it is done by calculating the proportion of rejected local null hypothesis to total predictions. More details on FDR approach can be found in Wilks (2006). In this study, FDR approach is employed for the KS test for the overall decision of rejection or nonrejection of the null hypothesis. All of these analyses are done by using the base package and “fdrtool” package in R programming.

4. Results

Here the results are presented based on the identified relationships among BFUs and each of the nine considered variables (Table 2). As seen in Figure 2a, the spatial variability of 5-day lag SSM is observed to range between 0.3% and 17% (volumetric basis) in the BFUs. Importantly, the NO and NE region BFUs retained higher soil moisture within the range of 4.5% to 17% 5 days prior to the bushfire incidents. In contrary, the SSM for the CE, SE, and SW region BFUs ranges from 0.3% to 8.5%. This low soil moisture (in the CE, SE, and SW BFUs) could have translated into lower dead fuel moisture, potentially leading to higher vulnerability of the litter and shrublands to bushfire in the corresponding regions (Qi et al., 2012). This is further validated by the two-sample KS test, where the null hypothesis is not rejected (Table 2) indicating that SSM contributes to bushfires in the overall NSW State.

Wind is one of the most critical variables governing the bushfire spread. Similar to SSM, average WS10 is also observed to be highly variable across the BFUs (Figure 2b). A lower magnitude of WS10 within the range of 3.1–8.3 ms^{−1} is observed for the SE region BFUs. On the other hand, the CE, NE, and NO region BFUs experienced a much higher WS10 (most BFUs experienced 15.5–28.0 ms^{−1}) for the duration of bushfire incidents at the BFUs. The BFUs in the SW region experienced WS10 in the range of 8.3–21.7 ms^{−1}. A more detailed analysis depicts that across the entire study area, approximately 90% of the BFUs experienced WS10 > 8.3 ms^{−1}. Furthermore, the two-sample KS test result indicates that the null hypothesis is not rejected (*p* value ≥ 0.05 as in Table 2), indicating both BFU area and WS10 follow the same distribution.

The average RH in the BFUs ranged from 18% to 67% for the bushfire duration at the BFUs (Figure 2c). Higher RH (within the range of 54–67%) is observed in the SE region BFUs, which are adjacent to the coastal region. Similarly, the BFUs which are adjacent to the coastal area in the NE region also experienced RH within the range of 42–54%. The high RH values in the coastal region relative to the inland BFUs are evident due to the oceanic water evaporation (Vicente-Serrano et al., 2018). According to the finding of Stephenson et al. (2015), regions have a higher probability of bushfire potential with RH values ≤65%, which is in the case of most of the BFUs over the entire region. The association of RH and the bushfires is further validated by the two-sample KS test where the null hypothesis is not rejected (*p* value > 0.05; Table 2), meaning that the samples derived from BFU area and RH follow the same distribution.

According to Figure 2d, seasonal average 6-month SPEI values indicate that all BFUs experienced droughts during the 2019–2020 bushfire season with magnitudes ranging from −0.70 to −2.50. The NE, CE, SE, and SW region BFUs experienced lower intensity drought (lower magnitude of negative value), most likely due to occasional sea breeze and erratic rainfall resulting from the pressure difference above sea and land (Curtis, 2019; Rezza Ferdiansyah et al., 2020). The BFUs located in the NO region are associated with higher magnitude (greater negative value) (intense) drought. This is consistent with the findings of Nolan et al. (2020), where during October the 6-month SPEI value was identified to be in the range of −1.1 to −2.6 in the NO and NE regions. Overall, the two-sample KS test also suggests the nonrejection of the null hypothesis, as seen in Table 2, which also demonstrates that bushfires are controlled by the drought

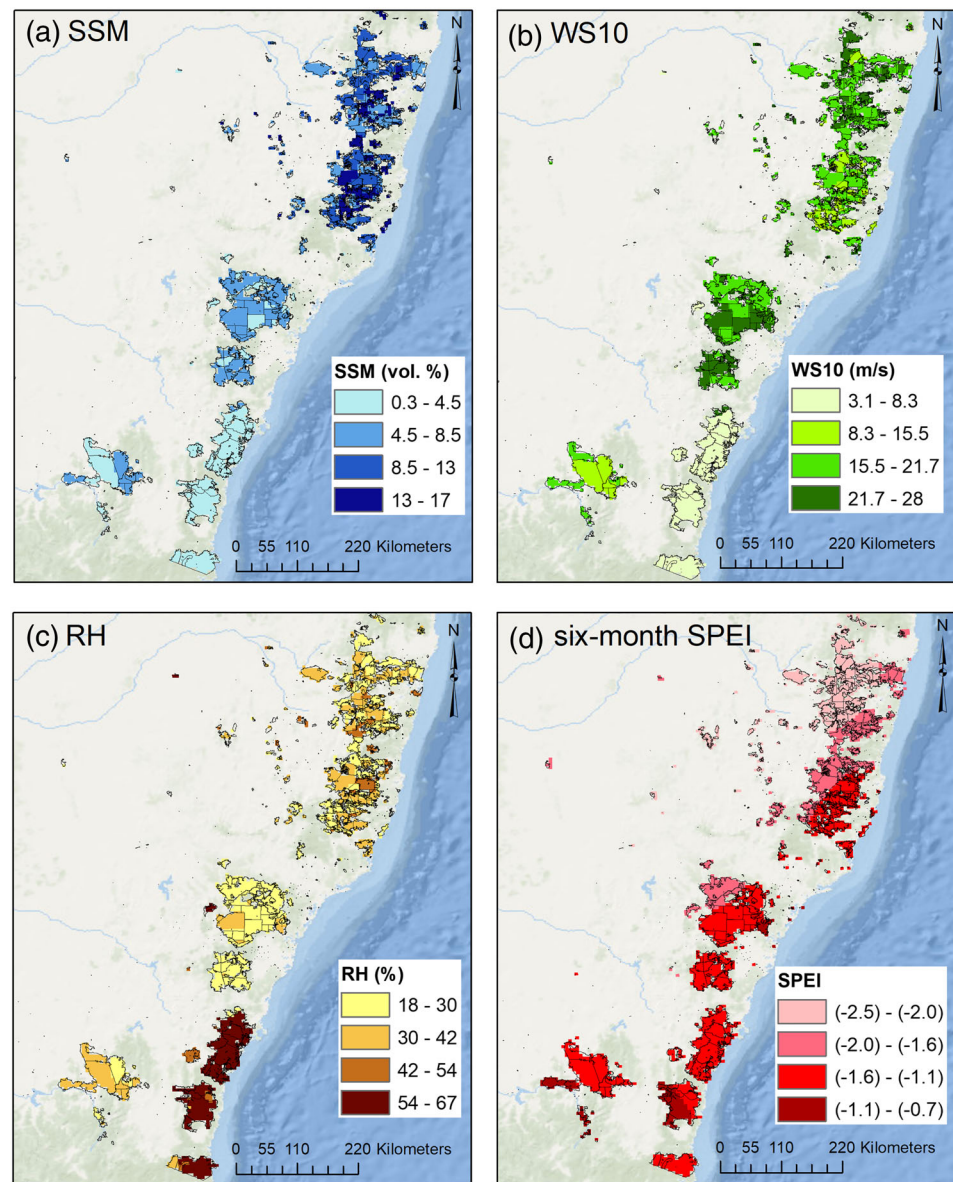


Figure 2. Spatial variability of (a) 5-day lag SSM (volumetric %), (b) average WS10 (ms^{-1}), (c) average RH (%), and (d) average 6-month SPEI for the bushfire duration considered in this study at the BFUs. Note that the bushfire duration refers to the days of bushfire continuation at each BFU; the attribute classification of each variable is done based on quantiles, which is displayed in the legend.

conditions in the BFUs. This is true given that droughts ensure fuel flammability as fuel moisture is depleted not only by the prolonged absence of rainfall but also by moisture outflux from tree litter/trees into the atmosphere (resulting from higher transpiration demand; Luo et al., 2016). Recent studies have also concluded that occasional torrential rainfall in conjunction with high winds promote fuel accumulation during droughts, as the herbaceous tree layers are more prone to peeling (Dimitrakopoulos et al., 2011; Russo et al., 2017). This not only elevates the risk of fire ignition but also easy fire propagation. Nonetheless, droughts intensified the bushfires in the BFUs considered in this study.

The analysis on HWs indicates that over 93% of the BFUs experience HWs in the season considered (i.e., September–December), except a few in the coastal region (for all months in Figure 3). The two-sample KS test result also suggests nonrejection of the null hypothesis, demonstrating both BFUs and number of HWs follow the same distribution (Table 2). This is possibly due to the favorable conditions for fire ignition created by the

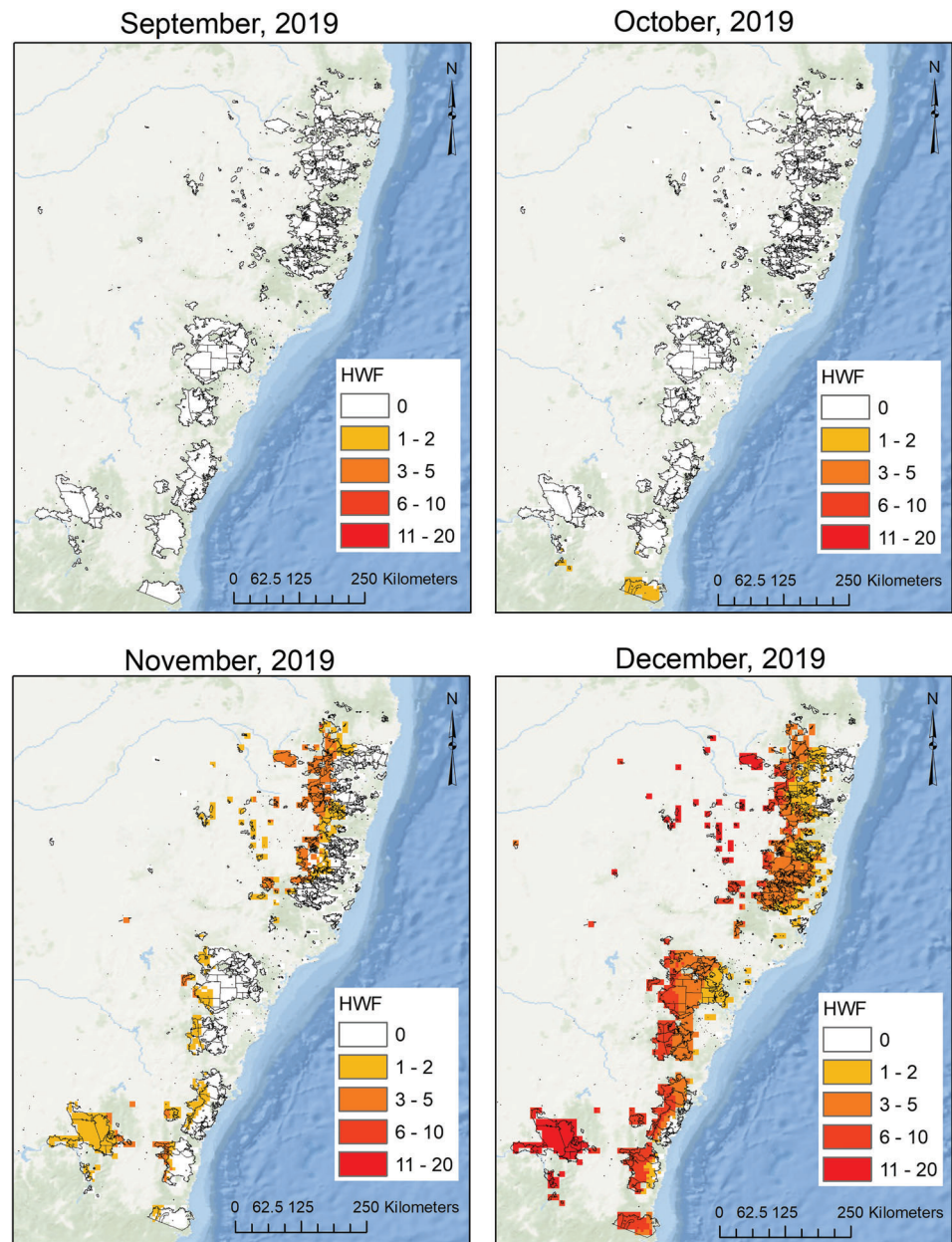


Figure 3. Spatial variability of the frequency of HW during September–December 2019 in the BFUs. Note: HWF denotes the HW frequency.

protracted higher temperatures, which is amplified by the lower RH and fuel moisture (discussed later) in the inland BFUs (where HWs are common in November). Median dry fuel moisture content below the threshold (14.6%) during October/November is also identified by Nolan et al. (2020) in the NE NSW region.

In addition to the two-sample KS test, an additional analysis to identify the frequency of the HWs in the BFUs is also done for the months of September–December. The results indicate that the SE and SW region BFUs experience profound HWs, which initiates from the spring season (October/November) and progresses through summer (December) (Figure 3). Noticeably during December in the SW BFUs, the number of HWs is over 10 (illustrating entire month experienced HWs). This is contrasting to the fact that the southern region is cooler compared to the northern region given the distance from the equator. However, the possible explanation for this abnormality is due to the hot wind mass traveling from the western desert toward

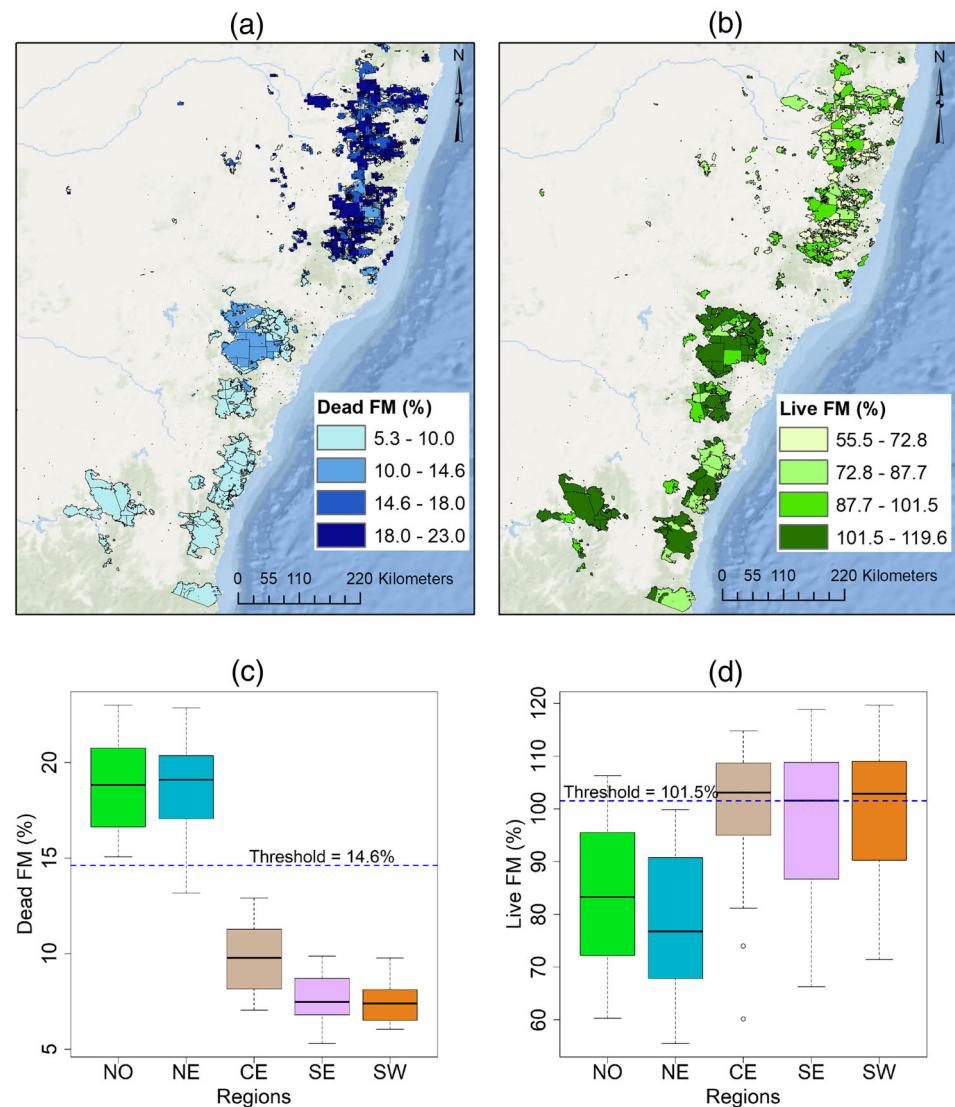


Figure 4. Spatial variability of (a) dead and (b) live fuel moisture at the BFUs. Region wise variation in the (c) dead and (d) live fuel moisture at the BFUs. (b) The fuel moisture which is temporally averaged only for the days of the bushfires at each BFU and (a) the dead fuel moisture retrieved from MODIS for the available day prior to the bushfire incidents at the BFUs; both live and dead fuel moisture are spatially averaged to represent the BFU scale fuel moisture values; the blue dashed line in panels (c) and (d) represents the critical threshold below which there is high likelihood of bushfire occurrence which is adopted from Nolan et al. (2016b).

the sea in the east (Shen et al., 2020). Additionally, in December, the NE region BFUs experienced short interval HWs. These early onsets of HW in the SE and SW region BFUs are in contrast to the findings from previous bushfire studies in southeast Australia where HWs reported to be pronounced only during December/January months (Cowan et al., 2014; Zhang et al., 2017). These findings exemplify the initiation of shifting in the HW seasonality which was predicted by Herold et al. (2018) under future climate. This will not only have implications on human health, agriculture, etc. but also exaggerating bushfires in the region.

The analysis of fine (10 h fuel) dead fuel moisture content suggests that NO and NE region BFUs contained dead fuel moisture in the range of 14.6–23.0% (Figure 4a). Although a few of the BFUs in the NE region also averaged dead fuel moisture between 10% and 14.6%, these BFU counts are minimal. BFUs in the CE region consisted of dead fuel moisture within the range of 5.3–14.6%. Similarly, for the SE and SW region BFUs, fuel moisture ranged from 5.3% to 10.0%. Figure 4c shows that the median dead fuel moisture content for the NO

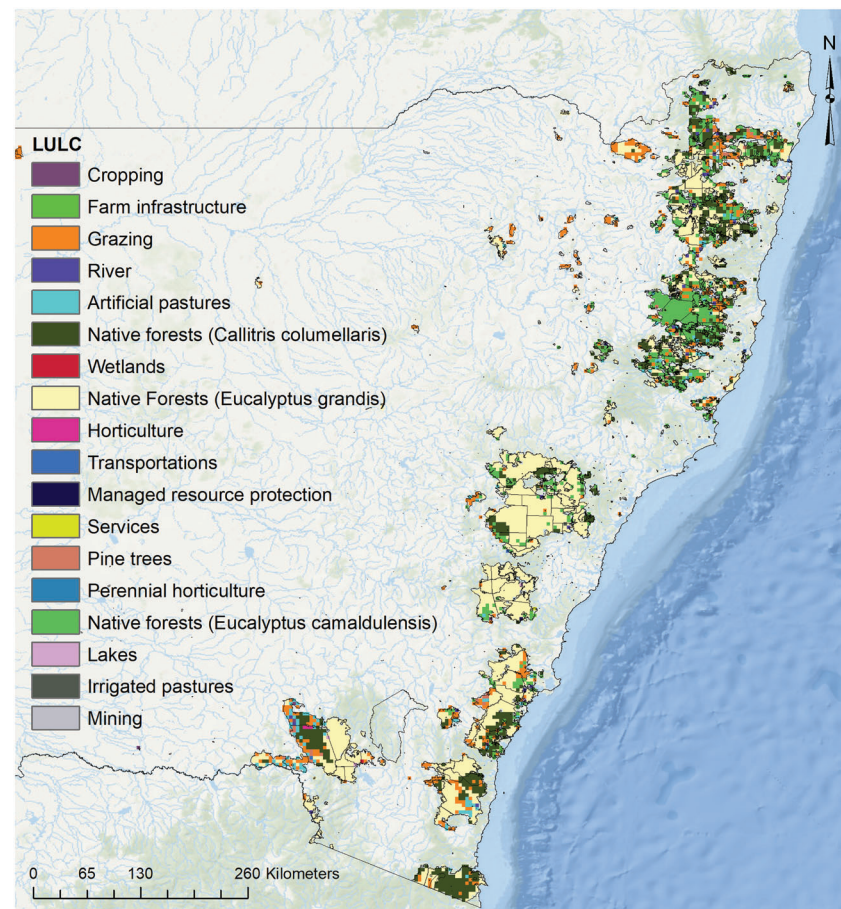


Figure 5. The LULC of the BFUs used in the analysis. Note: A majority of the BFUs comprise of different types of native forest which showed significant correlation among number of pixels within each BFU and BFU area.

and NE region BFUs is around 18.6% and 19.0%, respectively. Similarly, the median dead fuel moisture content for the SE and SW regions is around 7%. However, for the CE region, a slightly higher median dead fuel moisture content (~10%) is observed. While Nolan et al. (2016b), analyzed 2006/2007 and 2010/2011 bushfire seasons and identified a threshold of dead fuel moisture content (14.6%) in NSW state, below which there is a high likelihood of fire ignition, our results indicate that over 37% of the BFUs (mainly in the SE, SW, and CE regions) consisted of dead fuel moisture content below this threshold. This low dead fuel moisture, in conjunction with frequent and intense HW, may have caused majority of the bushfire incidents in the region. Furthermore, results of two-sample KS test also indicates the nonrejection of the null hypothesis that samples derived from the BFU area and dead fuel moisture content follow the same distribution.

The results of live fuel moisture are in contrast to the dead fuel moisture as lower magnitudes are observed for the NO and NE regions. The live fuel moisture in these BFUs ranges from 55.5% to 101.5%, whereas, 87.7% to 119.6% in the CE, SE, and SW region BFUs. Few of the BFUs are also noted to have live fuel moisture within the range of 72.8% to 87.7% in the CE, SE, and SW regions; however, the counts of these BFUs are very low. Nolan et al. (2016b) identified a live fuel moisture content threshold of 101.5% across the NSW state below which under favorable conditions, bushfires are highly probable. Across the entire study area, over 72% BFUs consisted of live fuel moisture below this threshold prior to the bushfire incidents. As mentioned, majority of these BFUs are located in the NE and NO region. Figure 4d also illustrates that the median live fuel moisture of the CE, SE and SW are over the threshold, whereas, for NO and NE regions the median values are approximately 84% and 76%, respectively. Furthermore, according to the results of two-sample KS test, the

Table 3
Kendall Rank Correlation Coefficient (τ) Among Number of Pixels in Each BFU and BFU Areas for Each Land Use Class

LULC	Kendall τ
Cropping	0.05
Farm Infrastructure	0.03
Grazing	0.36 ^a
River	−0.08
Artificial Pastures	0.12
Native forest (<i>Callitris columellaris</i>)	0.46 ^a
Wetlands	0.03
Native Forest (<i>Eucalyptus grandis</i>)	0.73 ^b
Horticulture	0.09
Transportations	0.01
Managed Resource Protection	0.06
Services	0.08
Pine trees	0.22
Perennial Horticulture	0.11
Native Forest (<i>Eucalyptus camaldulensis</i>)	0.44 ^a
Lakes	−0.03
Irrigated Pastures	0.02
Mining	0.05

^aSignificant at 0.05. ^bSignificant at 0.01.

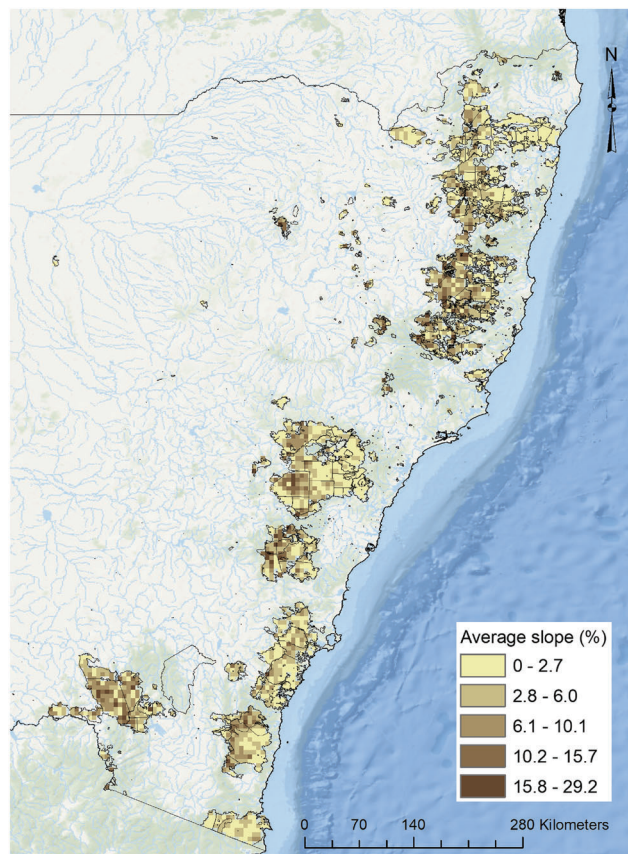


Figure 6. Slope (%) at the BFUs used in the analysis. Each pixel here in the figure depicts the range of slope; however, for the two-sample KS test, slope is averaged for each BFU and compared against the BFU area. Note: The attribute classification of the slope is done based on quantiles displayed in the legend.

null hypothesis of samples derived from the BFU area and dead fuel moisture follow same distribution is not rejected. Therefore, the dead fuel moisture is also identified to be a contributor to the bushfire spread.

The LULC map (Figure 5) indicates that a majority of the BFUs is comprised of forest land. The Kendall rank correlation coefficient (τ) calculated in this study (among the number of pixels in each BFU and BFU area) for each land use class (i.e., 18 classes in total) demonstrates that native forest lands are more susceptible to bushfire (Table 3). This is because these forest lands are generally dense with 50–80% crown cover (Specht, 1970) with typical tree heights ranging from 20 to 50 m. These tall and dense forests facilitate in faster-curing process for shrubs/grass by penetrating the radiant heat (Zhang et al., 2017) which is further accompanied by HW (discussed above). Another possible reason for the susceptibility of the native forests is due to the high concentration of extremely volatile and flammable oils (Barton et al., 1989) which vaporize rapidly under prolonged HW and ignites. Grazing land is also identified to be positively correlated to the BFUs. This can be explained by (1) the accumulation of ephemeral fuel due to human/animal interventions and (2) the radiated heat from the adjacent BFUs (as in Figure 5 where the BFUs with grazing are adjacent to native forest land) in conjunction with low RH is sufficient enough for fuel ignition. These findings are in line with those of Li et al. (2017) and Zhang et al. (2017) where grazing lands (semiarid regions of China) and native forests in NSW and Victoria States in Australia respectively are found more sensitive to bushfire. Additionally, Adams et al. (2020) also pointed that the recent bushfires were dominant in State Forest and National Parks which accounts for a majority in native forests.

Generally, slope plays a significant role in bushfire propagation (Boboulos & Purvis, 2009), yet the two-sample KS test reveals there is no statistically significant relationship between BFUs and their average slopes (Table 2). One possible reason for this conflicting result is due to the flat topography of the BFUs where a majority of the pixels (in this analysis) are in the range of 0–10.1% (Figure 6). Only a few of the pixels reflected values over 10.1% (pixels only covering in the Snowy and Blue Mountains which are above 1,000 m above sea level (a.s.l.) and are located around the CE region). It is to be noted that on a sloped terrain with wind favoring upslope direction, streamwise fire-induced negative pressure gradient is introduced. This leads to a higher magnitude of wind enhancement and consequently accelerating the bushfire front (Eftekharian et al., 2019). Another study has identified that the rate of fire propagation can increase up to 40 times with 30° (~57.7%) slope accompanied by the wind speed of 4 ms^{−1} relative to a flat topography (0% slope) and absence of wind (Boboulos & Purvis, 2009). Although these conclusions indicate the importance of slope, yet these are irrelevant in this study due to the absence of steep slopes in the BFUs.

5. Discussion and Conclusion

There is no denying that the 2019–2020 bushfire season in NSW, Australia, is one of the most catastrophic events which the State has ever experienced. This study uses empirical approaches to identifying variables that intensified the bushfire season. Previous studies on past bushfires have evaluated independent relationships among Australian bushfires

and climatic variables such as Lewis et al. (2020), Clarke et al. (2020), and Clarke and Evans (2019) and fuel moisture (Nolan et al., 2016a; de Dios et al., 2015). This study, on the other hand, evaluated all possible causes/factors contributing to the catastrophic bushfires accounting for climatic and geomorphic characteristics, which is also a novelty of this study. Additionally, apart from this study until now, there is no other study in literature that has investigated the detailed causes of the widespread 2019–2020 Australian bushfire.

While maximum temperature, fuel moisture, drought, and WS10 are usually the focus of research into causes of bushfires (Blanchi et al., 2014; Nolan et al., 2020; Sharples, McRae, et al., 2010), this study identified RH, HW, and SSM also as the key contributors to bushfire risk. Furthermore, certain land cover types such as native forests and grazing are more prone to bushfires. This latter finding is in line with that of Boer et al. (2020), who also identified 21% of the Australian temperate broadleaf and mixed forest biome (which typically accounts for the native eucalyptus trees) are burnt in the 2019–2020 bushfire season. Persistent drought and extreme high temperatures leading to HW are noticeable during September–December 2019. Even though interview-based studies from the past bushfire incidents have indicated that severe bushfires are due to prolonged drought in conjunction with high maximum temperatures and strong winds (Oloruntoba, 2013), the statistical tests conducted in this study also confirm it is true for the 2019–2020 bushfire season.

The findings of this study also suggest that several variables during and prior to the bushfire events are above/below the threshold at which bushfires are more likely to occur and spread. For instance, for the bushfire duration at the BFUs, WS10 is found to be above the threshold of 8.3 ms^{-1} (at which bushfires spread exponentially) as identified by Cruz and Alexander (2019). The high WS10 is noticed for over 78% of the BFUs over the entire study area. Similarly, as mentioned earlier, RH is noted to be below or close to the threshold of 65% for all BFUs at which there is a high likelihood of bushfire occurrence. Warmer temperatures and frequent HW throughout the BFUs in conjunction with low RH make the fuels more receptive to ignition (Sharples et al., 2016). Although in Australian context, currently, there is no study on the threshold of SSM at which the bushfire ignites or aid in spreading; however, according to this study, SSM is a critical component and needs attention. This is because SSM can have a contrasting effect in forested lands, high SSM facilitates increased fuel accumulation, whereas lower SSM can result in reduced fuel availability by limiting water in plants.

The analysis of fuel moisture indicates BFUs with high dead fuel moisture (over threshold) comprised of low live fuel moisture (below threshold) and vice versa. This is evident from the BFUs of NO and NE regions (dead fuel moisture over threshold); however, these BFUs have lower live fuel moisture (below threshold) and contrary in the case of CE, SE, and SW region BFUs. Although majority of the BFUs experienced dead fuel moisture lower than the threshold in this study, several prior studies have reported widespread bushfires with dead fuel moisture even as high as 30.8% (Nolan et al., 2016a; Nolan et al., 2016b). Remarkably, severe bushfires are also reported for dead fuel moisture below the threshold of 12.4–15.1% in boreal and subalpine forests of North America (Nash & Johnson, 1996). The threshold of 14.6% employed in this study corresponds to a vapor pressure deficit of $\sim 1.2 \text{ kPa}$, which is also consistent with the findings of Williams et al. (2015) who illustrated in USA burnt forest area increased rapidly with vapor pressure deficit within 1.2–1.4 kPa. This implies the threshold is not only limited to eucalypt forests but also a variety for forests worldwide.

In the case of live fuel moisture, several large BFUs ($>1,000 \text{ ha}$) are noted to have higher fuel moisture than the threshold value of 101.5%, particularly in the CE, SE, and SW regions. This finding is in contrast to that of a previous finding of Nolan et al. (2016b), where only small BFUs ($\leq 15 \text{ ha}$) are noted to have live fuel moisture value of higher than the threshold in case of 2006/2007 and 2010/2011 bushfire seasons. This conflicting result is likely due to the combined effect of frequent HW, low RH, and high WS10 in the large BFUs in 2019–2020 bushfire season, whereas the primary cause of the bushfires in the seasons (2006–2007 and 2010–2011) was due to lightning at localized and isolated BFUs (Dowdy & Mills, 2012). Moreover, a majority of the land cover in the recent bushfire season comprises native forests (eucalypt species) which inherit high flammability in contrast to the grazing land and shrublands in the previous fire seasons. Additionally, the bushfire risks in BFUs with high live fuel moisture is also aggravated by the critically low dead fuel moisture and SSM (as found in this study).

It is important to note that the fine dead fuel moisture is governed by ambient atmospheric conditions. Therefore, the transformation from wet to dry state for dead fuel moisture can be spontaneous. Live fuels,

on the other hand, need longer to transform as it is modulated by soil moisture. Due to the temporal variation in the wetting and drying cycles, dead fuels are generally available throughout the BFU seasons. Hence, dead fuel moisture condition is the first necessary precondition which triggers the bushfires followed by the live fuel moisture. Also, live fuel moisture is somehow dependent on dead fuel moisture. This is because even though dead fuel moisture may be below the critical threshold leading to ignition, the fire may not sustain if the live fuel moisture is above the threshold (Nolan et al., 2016a). Studies on these interdependencies among fuel moisture are critical and are worth to investigate in the future.

Modeling bushfires can aid in appropriate planning and management and are in practice since the 1950s. With the advancement of computational ability of modern computers, bushfire models have become complicated and account for several variables including the interactions among climate, vegetation, terrain, and land use (Boer et al., 2019; Clarke et al., 2019; Penman et al., 2013). Similarly, machine learning approaches are also widely accepted in bushfire applications such as Clarke et al. (2020) and Dutta et al. (2016). While employing such complex models over a large geographical domain is cumbersome, a simplistic model such as McArthur's FFDI index is generally more effective and hence operational in Australian context. One major issue with the FFDI index is that it accounts for the Drought Factor while employing simple water balance models such as Keetch-Byram Drought Index or Mount's Soil Dryness Index. Kumar and Dharssi (2017) discussed that both of these models are essentially poor in estimating shallow and root zone soil moisture when compared against in situ soil moisture measurements. Similarly, a different study by Holgate et al. (2017) introduced alternative soil moisture data (called antecedent precipitation index) instead of the integrated drought indices in the FFDI and the results indicated reduced low to moderate FDR and increased high FDR relative to the integrated FFDI approach. This study also reveals that the SSM is a critical information which is not well represented by the submodels in the FFDI, and therefore, it may lead to unrealistic results. Although FFDI is a versatile index and has been widely used for Australian conditions, yet some changes in it would make it more effective.

Slope is considered as a major contributor to bushfire since bushfire spread is exponentially related to the slope and is expressed as in Equation 5 (Noble et al., 1980).

$$R_{\theta} = R \times e^{0.069\theta} \quad (5)$$

where R_{θ} is rate of fire spread (km h^{-1}) at a given slope, θ is slope in degree, and R is rate of fire spread for flat ground (km h^{-1}). This implies for a fire spread rate of 5 km h^{-1} on a flat ground, with 10° ($\sim 17.6\%$) slope, the upslope fire spread rate elevates to 13.6 km h^{-1} . Additionally, slope may also modulate the wind directions at a given location, such as foehn-like occurrences with dry and warm winds on the lee side of mountains and hills which is common in the eastern region of Australia (Sharples, Mills, et al., 2010). While this may be a probable cause of the frequent HW in the BFUs, yet statistically no direct influence of slopes on the bushfire spread is observed at the BFUs.

A critical finding of this study is that native forests and grazing lands are at high bushfire risk, and hence, land use specific bushfire models or fire danger index is crucial. Although there are several land use specific fire spread rate models available which were developed for Australian biomes, the outputs of these models only illustrate the bushfire rate and do not explore the likelihood or probability of occurrence of a bushfire (Cruz et al., 2015a, 2015b). Furthermore, Australian bushfire research has come a long way in the development of bushfire models and a state-of-the-art model is Spark (Hilton et al., 2015). This model integrates climatic (such as temperature and wind) and geographical information (such as elevation and land use) to simulate the probable bushfire spread which implies it lacks in estimating a likelihood of fire ignition at a particular location and more specifically if any particular land use type is more vulnerable. This model is of course vital in devising management plans such as evacuation; however, it cannot answer some critical questions including (1) on which day (of a given season) a bushfire can ignite and spread and (2) what is the probability that a location will experience bushfire? In order to answer these questions, a better understanding of the physical processes controlling bushfire ignition is crucial. This study brings the science one-step closer to exploring answers to such questions.

It should be noted that the aim of this research is not to develop a new generalized index, rather to identify the variables which were overlooked in past studies (SSM, certain LULC, HW, live, and dead fuel moisture) and have contributed to the early onset of the 2019–2020 widespread bushfire season in NSW, Australia.

Given that the occurrence of droughts is uncertain (i.e., how/when/where drought frequency, duration, and intensity could change) (Kiem et al., 2016) and HW are projected to intensify (Perkins-Kirkpatrick et al., 2016) under climate change, developing a versatile index or improving the existing index can help with an accurate assessment of fire danger. Furthermore, future research should also seek to identify the tipping point of the fuel accumulation at which the aggregated fuel is more likely to ignite. This should include both field-scale studies along with the development of statistical/physical models. Moreover, fire severity is also an important aspect which this study did not account for and has a scope for future research. Considering existing bushfire research, this is relatively unexplored and imperative. Integrating all of this information in a single fire index will assist in (1) identifying periods of elevated bushfire risk and (2) developing appropriate bushfire planning and management.

Conflict of Interest

The authors declare no competing interests.

Data Availability Statement

The data sets used in this study are procured from different sources. Although the burnt area data used in this study is acquired through personal communication with the team leader of data management NSW Rural Fire Service (who is acknowledged), however, currently this data is also available at NSW data portal (<https://portal.data.nsw.gov.au>). The SSM data is obtained from Australian Landscape Water Balance model (<http://www.bom.gov.au/water/landscape/>). The WS10 data is available at NCEP/NCAR Reanalysis database (<https://www.esrl.noaa.gov/psd/data/>). The RH, maximum temperature, and vapor pressure deficit data sets are obtained from SILO data drill (<https://www.longpaddock.qld.gov.au/silo/>), and more details are available in Jeffrey et al. (2001). The 6-month SPEI data set is downloaded from Global SPEI database (<https://spei.csic.es/database.html>). The MODIS Terra MOD09A1 v6 data used to calculate VARI is obtained from USGS (<https://lpdaac.usgs.gov/products/mod09a1v006/>). The LULC data is procured from NSW Department of Planning, Industry and Environment (<https://datasets.seed.nsw.gov.au/dataset/nsw-land-use-2017-v1p2-f0ed>). Finally, the DEM data is retrieved from Geosciences Australia (<http://www.ga.gov.au/scientific-topics/national-location-information/digital-elevation-data>).

Acknowledgments

The authors would like to thank Mr. Nicholas Sharp, team leader of data management at NSW Rural Fire Service, for providing the burnt area data required for this study.

References

- Adams, M. A., Shadmanroodposhti, M., & Neumann, M. (2020). Causes and consequences of Eastern Australia's 2019–20 season of mega-fires: A broader perspective. *Global Change Biology*, 26. <https://doi.org/10.1111/gcb.15125>
- Alexander, L. V., & Arblaster, J. M. (2009). Assessing trends in observed and modelled climate extremes over Australia in relation to future projections. *International Journal of Climatology*, 29(3), 417–435. <https://doi.org/10.1002/joc.1730>
- Ambadan, J. T., Oja, M., Gedalof, Z., & Berg, A. A. (2020). Satellite-observed soil moisture as an Indicator of wildfire risk. *Remote Sensing*, 12(10), 1543. <https://doi.org/10.3390/rs12101543>
- Barton, M., F. A., Tjandra, J., & Nicholas, P. G. (1989). Chemical evaluation of volatile oils in eucalyptus species. *Journal of Agricultural and Food Chemistry*, 37(5), 1253–1257. <https://doi.org/10.1021/jf00089a011>
- Bessie, W. C., & Johnson, E. A. (1995). The relative importance of fuels and weather on fire behavior in subalpine forests. *Ecology*, 76(3), 747–762. <https://doi.org/10.2307/1939341>
- Blanchi, R., Leonard, J., Haynes, K., Opie, K., James, M., & Oliveira, F. D. d. (2014). Environmental circumstances surrounding bushfire fatalities in Australia 1901–2011. *Environmental Science and Policy*, 37, 192–203. <https://doi.org/10.1016/j.envsci.2013.09.013>
- Boboulos, M., & Purvis, M. R. I. (2009). Wind and slope effects on ROS during the fire propagation in East-Mediterranean pine forest litter. *Fire Safety Journal*, 44(5), 764–769. <https://doi.org/10.1016/j.firesaf.2009.03.006>
- Boer, M., Resco De Dios, V., Stefaniak, E., & Bradstock, R. (2019). A hydroclimatic model for the distribution of fire on Earth. *Biogeosciences Discussions*, 1–21. <https://doi.org/10.5194/bg-2019-441>
- Boer, M. M., Resco de Dios, V., & Bradstock, R. A. (2020). Unprecedented burn area of Australian mega forest fires. *Nature Climate Change*. <https://doi.org/10.1038/s41558-020-0716-1>
- Bowman, D. M. J. S., Balch, J. K., Artaxo, P., Bond, W. J., Carlson, J. M., Cochrane, M. A., et al. (2009). Fire in the earth system. *Science*, 324. <https://doi.org/10.1126/science.1163886>
- Bradstock, R., Penman, T., Boer, M., Price, O., & Clarke, H. (2014). Divergent responses of fire to recent warming and drying across south-eastern Australia. *Global Change Biology*, 20(5), 1412–1428. <https://doi.org/10.1111/gcb.12449>
- Bradstock, R. A., Nolan, R. H., Collins, L., Resco de Dios, V., Clarke, H., Jenkins, M., et al. (2020). A broader perspective on the causes and consequences of eastern Australia's 2019–20 season of mega-fires: A response to Adams et al. *Global Change Biology*, 26. <https://doi.org/10.1111/gcb.15111>
- Burton, J., Cawson, J., Noske, P., & Sheridan, G. (2019). Shifting states, altered fates: Divergent fuel moisture responses after high frequency wildfire in an obligate seeder eucalypt forest. *Forests*, 10(5), 436. <https://doi.org/10.3390/f10050436>
- Butler, B. W., Anderson, W., & Catchpole, E. A. (2007). Influence of slope on fire spread rate. In B. W. Butler, & W. Cook (Eds.), *The Fire Environment - Innovations, Management, and Policy* (pp. 75–82). Destin, FL: U.S. Department of Agriculture, Forest Service.

- Caccamo, G., Chisholm, L. A., Bradstock, R. A., Puotinen, M. L., & Pippen, B. G. (2012). Monitoring live fuel moisture content of heathland, shrubland and sclerophyll forest in south-eastern Australia using MODIS data. *International Journal of Wildland Fire*, 21(3), 257. <https://doi.org/10.1071/WF11024>
- Clarke, H., & Evans, J. P. (2019). Exploring the future change space for fire weather in southeast Australia. *Theoretical and Applied Climatology*, 136(1–2), 513–527. <https://doi.org/10.1007/s00704-018-2507-4>
- Clarke, H., Gibson, R., Cirulis, B., Bradstock, R. A., & Penman, T. D. (2019). Developing and testing models of the drivers of anthropogenic and lightning-caused wildfire ignitions in south-eastern Australia. *Journal of Environmental Management*, 235, 34–41. <https://doi.org/10.1016/j.jenvman.2019.01.055>
- Clarke, H., Lucas, C., & Smith, P. (2013). Changes in Australian fire weather between 1973 and 2010. *International Journal of Climatology*, 33(4), 931–944. <https://doi.org/10.1002/joc.3480>
- Clarke, H., Penman, T., Boer, M., Cary, G. J., Fontaine, J. B., Price, O., & Bradstock, R. (2020). The proximal drivers of large fires: A pyrogeographic study. *Frontiers in Earth Science*, 8, 90. <https://doi.org/10.3389/feart.2020.00090>
- Cowan, T., Purich, A., Perkins, S., Pezza, A., Bosch, G., & Sadler, K. (2014). More frequent, longer, and hotter heat waves for Australia in the twenty-first century. *Journal of Climate*, 27(15), 5851–5871. <https://doi.org/10.1175/JCLI-D-14-00092.1>
- Cruz, M. G., & Alexander, M. E. (2019). The 10% wind speed rule of thumb for estimating a wildfire's forward rate of spread in forests and shrublands. *Annals of Forest Science*, 76(2), 1–11. <https://doi.org/10.1007/s13595-019-0829-8>
- Cruz, M. G., Gould, J. S., Alexander, M. E., Sullivan, A. L., McCaw, W. L., & Matthews, S. (2015a). *A guide to rate of fire spread models for Australian vegetation*. Canberra ACT: CSIRO.
- Cruz, M. G., Gould, J. S., Alexander, M. E., Sullivan, A. L., McCaw, W. L., & Matthews, S. (2015b). Empirical-based models for predicting head-fire rate of spread in Australian fuel types. *Australian Forestry*, 78(3), 118–158. <https://doi.org/10.1080/00049158.2015.1055063>
- Curtis, S. (2019). Means and long-term trends of global coastal zone precipitation. *Scientific Reports*, 9(1), 1–9. <https://doi.org/10.1038/s41598-019-41878-8>
- Dai, A. (2013). Increasing drought under global warming in observations and models. *Nature Climate Change*, 3(1), 52–58. <https://doi.org/10.1038/nclimate1633>
- Deb, P., Kiem, A. S., & Willgoose, G. (2019). Mechanisms influencing non-stationarity in rainfall-runoff relationships in southeast Australia. *Journal of Hydrology*, 571, 749–764. <https://doi.org/10.1016/j.jhydrol.2019.02.025>
- de Dios, V. R., Fellows, A. W., Nolan, R. H., Boer, M. M., Bradstock, R. A., Domingo, F., & Goulden, M. L. (2015). A semi-mechanistic model for predicting the moisture content of fine litter. *Agricultural and Forest Meteorology*, 203, 64–73. <https://doi.org/10.1016/j.agrformet.2015.01.002>
- Dimitrakopoulos, A. P., Vlahou, M., Anagnostopoulou, C. G., & Mitsopoulos, I. D. (2011). Impact of drought on wildland fires in Greece: implications of climatic change? *Climatic Change*, 109(3–4), 331–347. <https://doi.org/10.1007/s10584-011-0026-8>
- Dosio, A. (2017). Projection of temperature and heat waves for Africa with an ensemble of CORDEX Regional Climate Models. *Climate Dynamics*, 49(1–2), 493–519. <https://doi.org/10.1007/s00382-016-3355-5>
- Dowdy, A. J., & Mills, G. A. (2012). Characteristics of lightning-attributed wildland fires in south-east Australia. *International Journal of Wildland Fire*, 21(5), 521. <https://doi.org/10.1071/WF10145>
- Dutta, R., Das, A., & Aryal, J. (2016). Big data integration shows Australian bush-fire frequency is increasing significantly. *Royal Society Open Science*, 3(2), 150241. <https://doi.org/10.1098/rsos.150241>
- Eftekharian, E., Ghodrat, M., He, Y., Ong, R. H., Kwok, K. C. S., Zhao, M., & Samali, B. (2019). Investigation of terrain slope effects on wind enhancement by a line source fire. *Case Studies in Thermal Engineering*, 14, 100467. <https://doi.org/10.1016/j.csste.2019.100467>
- Estes, B. L., Knapp, E. E., Skinner, C. N., Miller, J. D., & Preisler, H. K. (2017). Factors influencing fire severity under moderate burning conditions in the Klamath Mountains, northern California, USA. *Ecosphere*, 8(5), e01794. <https://doi.org/10.1002/ecs2.1794>
- Flannigan, M., Cantin, A. S., De Groot, W. J., Wotton, M., Newbery, A., & Gowman, L. M. (2013). Global wildland fire season severity in the 21st century. *Forest Ecology and Management*, 294, 54–61. <https://doi.org/10.1016/j.foreco.2012.10.022>
- Flannigan, M. D., Krawchuk, M. A., De Groot, W. J., Wotton, B. M., & Gowman, L. M. (2009). Implications of changing climate for global wildland fire. *International Journal of Wildland Fire*. <https://doi.org/10.1071/WF08187>
- Forootan, E., Khaki, M., Schumacher, M., Wulfmeyer, V., Mehrnegar, N., van Dijk, A. I. J. M., et al. (2019). Understanding the global hydrological droughts of 2003–2016 and their relationships with teleconnections. *Science of the Total Environment*, 650, 2587–2604. <https://doi.org/10.1016/j.scitotenv.2018.09.231>
- Giglio, L., Randerson, J. T., & van der Werf, G. R. (2013). Analysis of daily, monthly, and annual burned area using the fourth-generation global fire emissions database (GFED4). *Journal of Geophysical Research: Biogeosciences*, 118, 317–328. <https://doi.org/10.1002/jgrg.20042>
- Gitelson, A. A., Stark, R., Grits, U., Rundquist, D., Kaufman, Y., & Derry, D. (2002). Vegetation and soil lines in visible spectral space: A concept and technique for remote estimation of vegetation fraction. *International Journal of Remote Sensing*, 23(13), 2537–2562. <https://doi.org/10.1080/01431160110107806>
- Harrison, L., Funk, C., McNally, A., Shukla, S., & Husak, G. (2019). Pacific sea surface temperature linkages with Tanzania's multi-season drying trends. *International Journal of Climatology*, 39(6), 3057–3075. <https://doi.org/10.1002/joc.6003>
- Heritage, N. O. (2014). *Overview of New South Wales climate change*. Sydney, NSW: Government of New South Wales.
- Herold, N., Ekström, M., Kala, J., Goldie, J., & Evans, J. P. (2018). Australian climate extremes in the 21st century according to a regional climate model ensemble: Implications for health and agriculture. *Weather and Climate Extremes*, 20, 54–68. <https://doi.org/10.1016/j.wace.2018.01.001>
- Hilton, J., Hetherington, L., Miller, C., Sullivan, A., & Prakash, M. (2015). *The spark framework*. Clayton South, Victoria: CSIRO.
- Holgate, C. M., van Dijk, A. I. J. M., Cary, G. J., & Yebra, M. (2017). Using alternative soil moisture estimates in the McArthur Forest Fire Danger Index. *International Journal of Wildland Fire*, 26(9), 806. <https://doi.org/10.1071/WF16217>
- Ivanov, M., Warrach-Sagi, K., & Wulfmeyer, V. (2018). Field significance of performance measures in the context of regional climate model evaluation. Part 2: Precipitation. *Theoretical and Applied Climatology*, 132(1–2), 239–261. <https://doi.org/10.1007/s00704-017-2077-x>
- Jeffrey, S. J., Carter, J. O., Moodie, K. B., & Beswick, A. R. (2001). Using spatial interpolation to construct a comprehensive archive of Australian climate data. *Environmental Modelling and Software*, 16(4), 309–330. [https://doi.org/10.1016/S1364-8152\(01\)00008-1](https://doi.org/10.1016/S1364-8152(01)00008-1)
- Karoly, D. (2009). Bushfires and extreme heat in south-east Australia. In *RealClimate*. Retrieved from <http://www.realclimate.org/index.php/archives/2009/02/bushfires-and-climate/>
- Kiem, A. S., & Franks, S. W. (2004). Multi-decadal variability of drought risk, eastern Australia. *Hydrological Processes*, 18(11), 2039–2050. <https://doi.org/10.1002/hyp.1460>

- Kiem, A. S., Johnson, F., Westra, S., van Dijk, A., Evans, J. P., O'Donnell, A., et al. (2016). Natural hazards in Australia: Droughts. *Climatic Change*, 139(1), 37–54. <https://doi.org/10.1007/s10584-016-1798-7>
- King, A. D., Pitman, A. J., Henley, B. J., Ukkola, A. M., & Brown, J. R. (2020). The role of climate variability in Australian drought. *Nature Climate Change. Nature Research*. <https://doi.org/10.1038/s41558-020-0718-z>
- Krueger, E. S., Ochsner, T. E., Engle, D. M., Carlson, J. D., Twidwell, D., & Fuhlendorf, S. D. (2015). Soil moisture affects growing-season wildfire size in the southern great plains. *Soil Science Society of America Journal*, 79(6), 1567–1576. <https://doi.org/10.2136/sssaj2015.01.0041>
- Kumar, V., & Dharssi, I. (2017). *Evaluation of daily soil moisture deficit used in Australian forest fire danger rating system*. Melbourne: Bureau of Meteorology.
- Lewis, S. C., Blake, S. A. P., Trewin, B., Black, M. T., Dowdy, A. J., Perkins-Kirkpatrick, S. E., et al. (2020). Deconstructing factors contributing to the 2018 fire weather in Queensland, Australia. In S. C. Herring, N. Christidis, A. Hoell, M. P. Hoerling, P. A. Stott (Eds.), *Explaining extreme events of 2018 from a climate perspective* (1st ed., Vol. 101, pp. S115–S121). Boston, MA: Bulletin of the American Meteorological Society. <https://doi.org/10.1175/BAMS-ExplainingExtremeEvents2018.1>
- Li, Y., Zhao, J., Guo, X., Zhang, Z., Tan, G., & Yang, J. (2017). The influence of land use on the grassland fire occurrence in the northeastern inner Mongolia autonomous region, China. *Sensors (Switzerland)*, 17(3). <https://doi.org/10.3390/s17030437>
- Littell, J. S., McKenzie, D., Peterson, D. L., & Westerling, A. L. (2009). Climate and wildfire area burned in western U.S. ecoprovinces, 1916–2003. *Ecological Applications*, 19(4), 1003–1021. <https://doi.org/10.1890/07-1183.1>
- Liu, N., Wu, J., Chen, H., Xie, X., Zhang, L., Yao, B., et al. (2014). Effect of slope on spread of a linear flame front over a pine needle fuel bed: Experiments and modelling. *International Journal of Wildland Fire*, 23(8), 1087. <https://doi.org/10.1071/WF12189>
- Luo, Z., Guan, H., Zhang, X., Zhang, C., Liu, N., & Li, G. (2016). Responses of plant water use to a severe summer drought for two subtropical tree species in the central southern China. *Journal of Hydrology: Regional Studies*, 8, 1–9. <https://doi.org/10.1016/j.ejrh.2016.08.001>
- Marvel, K., & Bonfils, C. (2013). Identifying external influences on global precipitation. *Proceedings of the National Academy of Sciences of the United States of America*, 110(48), 19,301–19,306. <https://doi.org/10.1073/pnas.1314382110>
- Moritz, M. A., Morais, M. E., Summerell, L. A., Carlson, J. M., & Doyle, J. (2005). Wildfires, complexity, and highly optimized tolerance. *Proceedings of the National Academy of Sciences of the United States of America*, 102(50), 17,912–17,917. <https://doi.org/10.1073/pnas.0508985102>
- Nash, C. H., & Johnson, E. A. (1996). Synoptic climatology of lightning-caused forest fires in subalpine and boreal forests. *Canadian Journal of Forest Research*, 26(10), 1859–1874. <https://doi.org/10.1139/x26-211>
- Noble, I., Gill, A., & Bary, G. (1980). McArthur's fire-danger meters expressed as equations. *Australian Journal of Ecology*, 5(2), 201–203. <https://doi.org/10.1111/j.1442-9993.1980.tb01243.x>
- Nolan, R. H., Boer, M. M., Resco De Dios, V., Caccamo, G., & Bradstock, R. A. (2016a). Large-scale, dynamic transformations in fuel moisture drive wildfire activity across southeastern Australia. *Geophysical Research Letters*, 43, 4229–4238. <https://doi.org/10.1002/2016GL068614>
- Nolan, R. H., Boer, M. M., Collins, L., Resco de Dios, V., Clarke, H., Jenkins, M., et al. (2020). Causes and consequences of eastern Australia's 2019–20 season of mega-fires. *Global Change Biology*, 26(3), 1039–1041. <https://doi.org/10.1111/gcb.14987>
- Nolan, R. H., Resco de Dios, V., Boer, M. M., Caccamo, G., Goulden, M. L., & Bradstock, R. A. (2016b). Predicting dead fine fuel moisture at regional scales using vapour pressure deficit from MODIS and gridded weather data. *Remote Sensing of Environment*, 174, 100–108. <https://doi.org/10.1016/j.rse.2015.12.010>
- O'Donnell, A. J., Boer, M. M., McCaw, W. L., & Grierson, P. F. (2011). Climatic anomalies drive wildfire occurrence and extent in semi-arid shrublands and woodlands of southwest Australia. *Ecosphere*, 2(11). <https://doi.org/10.1890/ES11-00189.1>
- Oloruntoba, R. (2013). Plans never go according to plan: An empirical analysis of challenges to plans during the 2009 Victoria bushfires. *Technological Forecasting and Social Change*, 80, 1674–1702. <https://doi.org/10.1016/j.techfore.2012.12.002>
- Penman, T. D., Bradstock, R. A., & Price, O. (2013). Modelling the determinants of ignition in the Sydney Basin, Australia: Implications for future management. *International Journal of Wildland Fire*, 22(4), 469. <https://doi.org/10.1071/WF12027>
- Perkins-Kirkpatrick, S. E., White, C. J., Alexander, L. V., Argüeso, D., Bosch, G., Cowan, T., et al. (2016). Natural hazards in Australia: Heatwaves. *Climatic Change*, 139(1), 101–114. <https://doi.org/10.1007/s10584-016-1650-0>
- Qi, Y., Dennison, P. E., Spencer, J., & Riaño, D. (2012). Monitoring live fuel moisture using soil moisture and remote sensing proxies. *Fire Ecology*, 8(3), 71–87. <https://doi.org/10.4996/fireecology.0803071>
- Rezza Ferdiansyah, M., Inagaki, A., & Kanda, M. (2020). Detection of sea-breeze inland penetration in the coastal-urban region using geostationary satellite images. *Urban Climate*, 31, 100586. <https://doi.org/10.1016/j.uclim.2020.100586>
- Roach, J. (2020). Australia wildfire economic damages and losses to reach \$110 billion. In *AccuWeather*. State College, PA: AccuWeather. Retrieved from <https://www.accuweather.com/en/business/australia-wildfire-economic-damages-and-losses-to-reach-110-billion/657235>
- Russo, A., Gouveia, C. M., Páscoa, P., Dacamara, C. C., Sousa, P. M., & Trigo, R. M. (2017). Assessing the role of drought events on wildfires in the Iberian Peninsula. *Agricultural and Forest Meteorology*, 50–59. <https://doi.org/10.1016/j.agrformet.2017.01.021>
- Russo, S., Dosio, A., Graversen, R. G., Sillmann, J., Carrao, H., Dunbar, M. B., et al. (2014). Magnitude of extreme heat waves in present climate and their projection in a warming world. *Journal of Geophysical Research: Atmospheres*, 119, 12,500–12,512. <https://doi.org/10.1002/2014JD022098>
- Sanderson, B. M., & Fisher, R. A. (2020). A fiery wake-up call for climate science. *Nature Climate Change. Nature Research*, 10. <https://doi.org/10.1038/s41558-020-0707-2>
- Schulte, M. L., McLaughlin, D. L., Wurster, F. C., Varner, J. M., Stewart, R. D., Aust, W. M., et al. (2019). Short- and long-term hydrologic controls on smouldering fire in wetland soils. *International Journal of Wildland Fire*, 28(3), 177. <https://doi.org/10.1071/WF18086>
- Sharples, J. J., McRae, R. H. D., & Weber, R. O. (2010). Wind characteristics over complex terrain with implications for bushfire risk management. *Environmental Modelling and Software*, 25(10), 1099–1120. <https://doi.org/10.1016/j.envsoft.2010.03.016>
- Sharples, J. J., Cary, G. J., Fox-Hughes, P., Mooney, S., Evans, J. P., Fletcher, M. S., et al. (2016). Natural hazards in Australia: Extreme bushfire. *Climatic Change*, 139(1), 85–99. <https://doi.org/10.1007/s10584-016-1811-1>
- Sharples, J. J., Mills, G. A., McRae, R. H. D., & Weber, R. O. (2010). Foehn-like winds and elevated fire danger conditions in southeastern Australia. *Journal of Applied Meteorology and Climatology*, 49(6), 1067–1095. <https://doi.org/10.1175/2010JAMC2219.1>
- Shen, X., Wang, L., & Osprey, S. (2020). The Southern Hemisphere sudden stratospheric warming of September 2019. *Science Bulletin*, 65. <https://doi.org/10.1016/j.scib.2020.06.028>
- Specht, R. (1970). Vegetation. In G. Leeper (Ed.), *The Australian Environment* (pp. 44–67). Melbourne: Melbourne University Press.

- Stephenson, A. G., Shaby, B. A., Reich, B. J., & Sullivan, A. L. (2015). Estimating spatially varying severity thresholds of a Forest fire danger rating system using max-stable extreme-event modeling. *Journal of Applied Meteorology and Climatology*, 54(2), 395–407. <https://doi.org/10.1175/JAMC-D-14-0041.1>
- TV10. (2020). *Estimated 1.25 billion animals killed in Australian bushfires* | WBNS-10TV Columbus, Ohio | Columbus News, Weather & Sports. Columbus, OH: 10TV. Retrieved from <https://www.10tv.com/article/estimated-125-billion-animals-killed-australian-bushfires-2020-jan>
- Verdon, D. C., Kiem, A. S., & Franks, S. W. (2004). Multi-decadal variability of forest fire risk - eastern Australia. *International Journal of Wildland Fire*, 13(2), 165. <https://doi.org/10.1071/WF03034>
- Vicente-Serrano, S. M., Nieto, R., Gimeno, L., Azorin-Molina, C., Drumond, A., el Kenawy, A., et al. (2018). Recent changes of relative humidity: Regional connections with land and ocean processes. *Earth System Dynamics*, 9, 915–937. <https://doi.org/10.5194/esd-9-915-2018>
- Weber, D., Moskwa, E., Robinson, G. M., Bardsley, D. K., Arnold, J., & Davenport, M. A. (2019). Are we ready for bushfire? Perceptions of residents, landowners and fire authorities on Lower Eyre Peninsula, South Australia. *Geoforum*, 107, 99–112. <https://doi.org/10.1016/j.geoforum.2019.10.006>
- Wilks, D. S. (2006). On “field significance” and the false discovery rate. *Journal of Applied Meteorology and Climatology*, 45(9), 1181–1189. <https://doi.org/10.1175/JAM2404.1>
- Williams, A. P., Seager, R., Macalady, A. K., Berkelhammer, M., Crimmins, M. A., Swetnam, T. W., et al. (2015). Correlations between components of the water balance and burned area reveal new insights for predicting forest fire area in the southwest United States. *International Journal of Wildland Fire*, 24(1), 14. <https://doi.org/10.1071/WF14023>
- Wu, R., & Kinter, J. L. III (2009). Analysis of the relationship of U.S. droughts with SST and soil moisture: Distinguishing the time scale of droughts. *Journal of Climate*, 22, 4520–4538. <https://doi.org/10.1175/2009JCLI2841.1>
- Yeung, J. (2020). *Australia wildfires: Here's what you need to know about the deadly blazes*—CNN. Atlanta, GA: CNN. Retrieved from <https://www.cnn.com/2020/01/01/australia/australia-fires-explainer-intl-hnk-scli/index.html>
- Zhang, Y., Lim, S., & Sharples, J. J. (2017). Effects of climate on the size of wildfires in the Eucalyptus camaldulensis forests and the dry lands of the Riverina Bioregion, Australia. *Forest Ecology and Management*, 401, 330–340. <https://doi.org/10.1016/j.foreco.2017.07.009>